Evolution of moth sex pheromone composition by a single amino acid substitution in a fatty acid desaturase

Aleš Buček[a,1], Petra Matoušková[b,1], Heiko Vogel[c], Petr Šebesta[a], Ullrich Jahn[a], Jerrit Weißflog[d], Aleš Svatoš[a,d,2], and Iva Pichová[a,2]

[a]Institute of Organic Chemistry and Biochemistry, Academy of Sciences of the Czech Republic, 166 10 Prague 6, Czech Republic; [b]Faculty of Pharmacy, Charles University in Prague, 500 05 Hradec Králové, Czech Republic; [c]Max Planck Institute for Chemical Ecology, Department of Entomology, D-07745, Jena, Germany; and [d]Max Planck Institute for Chemical Ecology, Mass Spectrometry Group, D-07745, Jena, Germany

Edited by Jerrold Meinwald, Cornell University, Ithaca, NY, and approved September 3, 2015 (received for review July 23, 2015)

For sexual communication, moths primarily use blends of fatty acid derivatives containing one or more double bonds in various positions and configurations, called sex pheromones (SPs). To study the molecular basis of novel SP component (SPC) acquisition, we used the tobacco hornworm (*Manduca sexta*), which uses a blend of mono-, di-, and uncommon triunsaturated fatty acid (3UFA) derivatives as SP. We identified pheromone-biosynthetic fatty acid desaturases (FADs) *Msex*D3, *Msex*D5, and *Msex*D6 abundantly expressed in the *M. sexta* female pheromone gland. Their functional characterization and in vivo application of FAD substrates indicated that *Msex*D3 and *Msex*D5 biosynthesize 3UFAs via *E*/*Z*14 desaturation from diunsaturated fatty acids produced by previously characterized *Z*11-desaturase/conjugase *Msex*D2. Site-directed mutagenesis of sequentially highly similar *Msex*D3 and *Msex*D2 demonstrated that swapping of a single amino acid in the fatty acyl substrate binding tunnel introduces *E*/*Z*14-desaturase specificity to mutated *Msex*D2. Reconstruction of FAD gene phylogeny indicates that *Msex*D3 was recruited for biosynthesis of 3UFA SPCs in *M. sexta* lineage via gene duplication and neofunctionalization, whereas *Msex*D5 representing an alternative 3UFA-producing FAD has been acquired via activation of a presumably inactive ancestral *Msex*D5. Our results demonstrate that a change as small as a single amino acid substitution in a FAD enzyme might result in the acquisition of new SP compounds.

fatty acid desaturase | *Manduca sexta* | sex pheromone biosynthesis | pheromone evolution | substrate specificity

Sex pheromones (SPs) are a diverse group of chemical compounds that are central to mate-finding behavior in insects (1). Variation in SP composition between closely related species and among populations is well documented. Despite this variation, SPs are presumed to be under strong stabilizing selection, and thus the genetic mechanisms driving SP diversification represented an enigma (2). Research on SPs in moths (Insecta: Lepidoptera) helped establish the hypothesis of asymmetric tracking as a major driving force in SP diversification. In this scenario, abrupt changes in female SP composition via a shift in component ratio or the inclusion or loss of a component result in a distinct SP that attracts males with more broadly or differentially tuned SP preference (3). Assortative mating, the preferential mating of females producing a novel SP with males attracted to this SP, restricts gene flow between subpopulations with differing SP compositions. This can ultimately lead to speciation and fixation of novel communication channels (4). Work in insect models such as wasps (5), fruit flies (6), and especially moths (7–9) is helping uncover the genetic basis of SP diversification.

In the majority of moth species, females use species-specific mixtures of SP components (SPCs) consisting of volatile fatty acid (FA) derivatives to attract conspecific males at long range. These SPCs are predominantly long-chain aliphatic (C12–C18) acetates, alcohols, or aldehydes containing zero to three double bonds of various configurations at different positions along the carbon backbone (10). Pheromone biosynthesis involves modifications of fatty acyl substrates, such as chain shortening and elongation, reduction, acetylation, oxidation, and desaturation (11). SP biosynthetic enzymes [i.e., FA reductases (8), FA chain-shortening enzymes (12, 13), and particularly FA desaturases (FADs) (7, 9, 14–17)] are the most commonly discovered traits underlying SP divergence in moths.

Manduca sexta females attract males by releasing an SP containing in addition to mono- and diunsaturated aldehydes, which are typical structural themes in SPs of Bombycoidea moths (10), also uncommon conjugated triunsaturated aldehydes. The production of triunsaturated SPCs represents an easily traceable phenotype, thus making *M. sexta* a convenient yet unexploited model organism for unraveling the mechanisms of chemical communication evolution via novel SPC recruitment. In our previous attempts to decipher the desaturation pathway leading to triunsaturated SPC FA precursors (3UFAs), we identified the *Msex*D2 desaturase, which exhibits *Z*11-desaturase and conjugase (1,4-dehydrogenase) activity and participates in stepwise production of monounsaturated (1UFA) and diunsaturated (2UFA) SPC precursors. The terminal desaturation step resulting in the third conjugated double bond remained, however, elusive (18, 19).

Here, we isolated and functionally characterized FAD genes abundantly and specifically expressed in the pheromone gland

Significance

The diversity of sex pheromones (SPs) is pivotal to insect reproductive isolation and speciation. However, knowledge of molecular mechanisms of pheromone evolution is limited. The *Manduca sexta* SP contains unique triunsaturated fatty acid (3UFA) derivatives and represents thus a suitable model for the investigation of chemical communication evolution via recruitment of novel SP components. Here, we demonstrate that gene duplication and a single amino acid substitution in fatty acid desaturase (FAD) catalyzing production of diunsaturated moth pheromone precursors is sufficient for acquisition of 3UFA SP component precursors. Our study indicates that the potential for change in the moth pheromone composition is underlined by the inherent evolvability of pheromone biosynthetic FADs.

Author contributions: A.B., U.J., A.S., and I.P. designed research; A.B., P.M., H.V., P.S., J.W., and A.S. performed research; A.B., P.M., H.V., A.S., and I.P. analyzed data; and A.B., H.V., U.J., A.S., and I.P. wrote the paper.

The authors declare no conflict of interest.

This article is a PNAS Direct Submission.

Data deposition: The sequences reported in this paper have been deposited in the GenBank database (accession nos. AM158251 and KP890026–KP890030).

[1]A.B. and P.M. contributed equally to this work.

[2]To whom correspondence may be addressed. Email: svatos@ice.mpg.de or iva.pichova@uochb.cas.cz.

This article contains supporting information online at www.pnas.org/lookup/suppl/doi:10.1073/pnas.1514566112/-/DCSupplemental.

(PG) capable of producing 3UFA pheromone precursors and demonstrated the biosynthesis of 3UFAs from 2UFAs. We used site-directed mutagenesis of *M. sexta* FADs and identified a minimal structure motif leading to acquisition of new desaturase specificities. The reconstructed evolutionary relationship of moth FADs demonstrated that the 3UFA pheromone precursors in *M. sexta* were acquired via (*i*) activation of a presumably inactive ancestral FAD gene and/or (*ii*) duplication of an ancestral FAD gene producing 1UFA and 2UFA SPC precursors followed by functional diversification of an FAD duplicate.

Results

Identification of FADs Abundant in the Pheromone Gland. To select candidate FAD genes involved in pheromone biosynthesis, we performed RNA sequencing of *M. sexta* female PGs, the site of pheromone biosynthesis (19), as well as nonpheromone-producing tissues (female fat body, female labial palps, and larval midgut). We identified 14 desaturase transcripts, of which 4 were abundant and enriched in the PG according to normalized expression values (RPKM, reads per kilobase of transcript per million mapped reads): *Msex*D2, a previously characterized Z11-desaturase/conjugase involved in sequential biosynthesis of 1UFA and 2UFA pheromone precursors (18), and three FAD gene products, *Msex*D3, *Msex*D5 and *Msex*D6 (Fig. 1). According to the RPKM values, *Msex*D2 and *Msex*D3 were among the 100 most abundant transcripts in *M. sexta* PG, ranking 12th and 4th, respectively (Dataset S1). A transcript coding for fatty acyl reductase, a gene presumably involved in reduction of fatty acyl pheromone precursors to aldehydic pheromones, was also abundantly expressed (Dataset S1).

The ORF of *Msex*D3 (GenBank accession no. AM158251) encodes a 341-aa protein containing conserved structural features of membrane FADs, that is, three histidine-rich motifs involved in coordination of two iron atoms in the enzyme active site and four transmembrane helices (20, 21). In the *M. sexta* Official Gene Set 2.0 (OGS 2.0; www.agripestbase.org/manduca/), the *Msex*D2 and *Msex*D3 genes are tandemly organized in the genome, located on the same scaffold and separated by 7 kbp (scaffold00070: 983841–985384 and 993705–995505, respectively). Together with the high sequence identity of *Msex*D2 and *Msex*D3 (91% in the homologous 321-aa region, *SI Appendix*, Fig. S1) these data indicate that *Msex*D2 and *Msex*D3 emerged via a recent gene duplication event from an ancestral FAD gene.

Four *Msex*D5 ORF variants (*Msex*D5a–*Msex*D5d) that code for highly similar proteins sharing at least 92% sequence identity were amplified from the *M. sexta* female abdominal tips (ATs) cDNA libraries (GenBank accession nos. KP890027–KP890030) (*SI Appendix*, Fig. S2). These sequences presumably represent allelic variants of a single *Msex*D5 gene, supported by the presence of a single *Msex*D5 gene copy in the *M. sexta* OGS 2.0 (scaffold 00367: 113800–112161). The *Msex*D5 consensus sequence shares moderate protein sequence identity with *Msex*D2 and *Msex*D3 (49.8 and 51.7%, respectively) (*SI Appendix*, Fig. S3).

*Msex*D6 is the least abundantly expressed PG-specific FAD (Fig. 1). Compared with all predicted *M. sexta* FADs, the *Msex*D6 coding region (GenBank accession no. KP890026) exhibits the highest protein sequence identity to *Msex*D2 and *Msex*D3 (68.0 and 71.5%, respectively) (*SI Appendix*, Fig. S3).

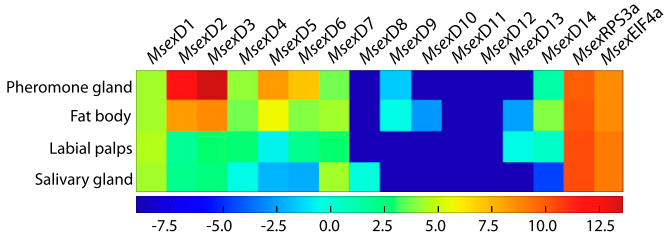

Fig. 1. Heat map indicating transcript abundances of *Msex*D1-*Msex*D14 along with abundances of housekeeping genes Msex-RPS3a and Msex-EIF4a. Transcript abundances are expressed as log2 transformed normalized values (RPKM) across various tissues obtained from virgin *M. sexta* females (pheromone gland, fat body, and labial palps) and from larvae (salivary glands).

Functional Characterization of *Msex*D3, *Msex*D5, and *Msex*D6. We selected *Msex*D3, *Msex*D5a–d, and *Msex*D6 as promising candidate FADs producing 3UFA precursors of SPCs based on their abundant and specific expression in the PG. For functional characterization of FADs, we initially attempted to express the candidate FADs in the *elo1Δ ole1Δ Saccharomyces cerevisiae* strain, which is deficient in the fatty acid desaturation and medium-chain fatty acyl elongation step (22), to eliminate interfering yeast FA metabolites. However, only trace levels of novel unsaturated FAs, detected in the form of FA methyl esters (FAMEs), were biosynthesized in this expression system. Therefore, we characterized FADs in *S. cerevisiae* strain W303, which has a single FAD with *Z*9 specificity and an active FA elongase system. To distinguish the interfering products of natural yeast FA metabolism from the specific products of *M. sexta* FADs, we performed a series of control cultivations of yeast bearing an empty expression plasmid (Fig. 2 and *SI Appendix*, Fig. S4).

To test the ability of *Msex*D3 to produce 3UFAs, we supplemented the yeast cultivation medium with the presumed 3UFA precursor *E*10,*E*12-16:2. This resulted in production of a 1:7 mixture of *E*10,*E*12,*E*14-16:3 and *E*10,*E*12,*Z*14-16:3 (Fig. 2*D*). Monounsaturated FAs were detected as additional specific products of *Msex*D3, that is, *Z*11-16:1, *Z*11-14:1, and *E*11-14:1. *Z*11-16:1, an FA precursor of a monounsaturated pheromone component, was produced in a significantly lower ($P < 0.05$) amount in the *Msex*D3-expressing strain compared with the *Msex*D2-expressing strain ($0.9 \pm 0.5\%$ and $10.6 \pm 0.2\%$, respectively) (Fig. 2). In the *Msex*D3-expressing strain, additional C16:1 and C16:2 FAs with *E*/*Z*13 double bonds were detected. These FAs were biosynthesized not via direct *E*/*Z*13 desaturation but rather by elongation of *E*/*Z*11-14:1, presumably catalyzed by yeast fatty acyl elongase Elo1p (22), followed by a second round of *Z*11 desaturation, as demonstrated by a series of cultivation experiments (*SI Appendix*, Fig. S4). In contrast to *Msex*D2, *Msex*D3 did not exhibit conjugase activity; it did not desaturate the supplemented *Z*11-16:1 to *E*10,*E*12-16:2 or *E*10,*Z*12-16:2 (Fig. 2*C*). MTAD (4-methyl-1,2,4-triazoline-3,5 dione) derivatization was used to confirm the presence or absence of FAMEs with conjugated double bonds (*SI Appendix*, Figs. S4*D* and S5).

The *Msex*D5a–*Msex*D5d variants also produced *E*10,*E*12,*E*14:16-3 and *E*10,*E*12,*Z*14-16:3 (in an ∼3:1 ratio) from *E*10,*E*12-16:2 added to the cultivation medium, indicating that all *Msex*D5 variants exhibit *E*/*Z*14-desaturase specificity (Fig. 2*D* and *SI Appendix*, Fig. S6). Therefore, a single FAD variant, *Msex*D5a (hereafter referred to as *Msex*D5), was used in subsequent experiments. *Msex*D5 substrate specificity was assayed by supplementing the cultivation media of *Msex*D5-expressing yeast with *Z*11-16:1-methyl ester. Although no *E*10,*E*12-16:2 or *E*10,*Z*12-16:2 products were detected, we did detect small quantities of *Z*11,*E*13-16:2, demonstrating *E*13 specificity and lack of conjugase activity in *Msex*D5 (Fig. 2*C* and *SI Appendix*, Fig. S4). In contrast to *Msex*D3, *Msex*D5 did not produce *E*11-14:1 or *Z*11-14:1 (Fig. 2*A*), and *Z*11-16:1 was detected in the *Msex*D5-expressing yeast strain at a level comparable to that in the empty strain, indicating that *Msex*D5 lacks *Z*11-desaturase activity with a 16:0 substrate (Fig. 2*B*).

*Msex*D6 did not produce 3UFAs when supplemented with *E*10,*E*12-16:2; however, it produced a substantial amount of *Z*11-18:1 ($12.3 \pm 0.2\%$), an FA with a hydrocarbon backbone identical to the *M. sexta* SPC *Z*11-18:1-aldehyde (*SI Appendix*, Fig. S7). The configuration of the Δ11 double bond was tentatively identified as *Z*11 based on the matching retention time of the *Msex*D6 product with a minor Δ11-18:1 FAME presumably resulting from FA elongation of abundant *Z*9-16:1 in all yeast strains (*SI Appendix*, Fig. S7). Additionally, *Msex*D6 produced $1.3 \pm 0.3\%$ *Z*11-16:1 (Fig. 2*B*).

Analysis of Isotopically Labeled and Natural FAs in *M. sexta* Female AT. To complement the functional characterization of FADs in the yeast expression system and identify the in vivo substrates

CHEMISTRY

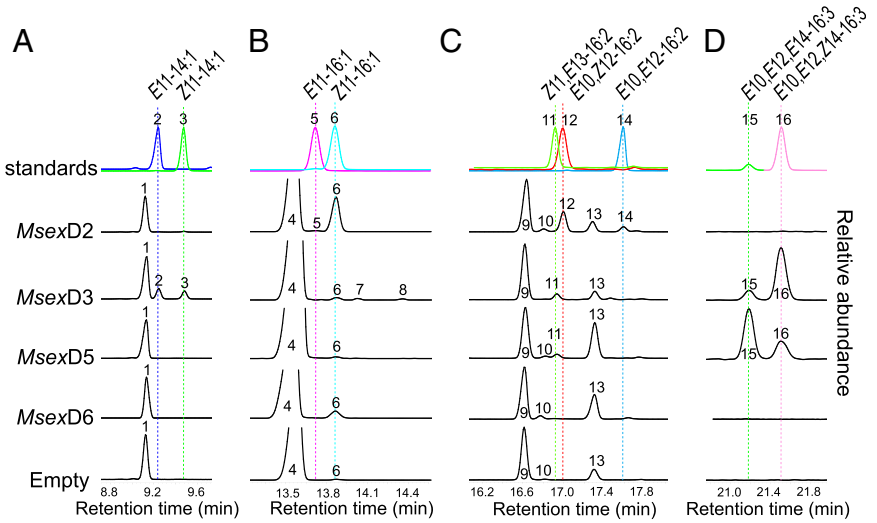

Fig. 2. GC/MS analyses of extracts from yeast cells expressing *M. sexta* desaturases. Extracts from yeasts expressing *Msex*D2, *Msex*D3, *Msex*D5, and *Msex*D6 were compared with extracts from yeasts transformed with an empty plasmid. Chromatograms are displayed as extracted ion chromatograms at (*A*) *m/z* 240, corresponding to the molecular ion ($M^{+\bullet}$) of 14:1; (*B*) *m/z* 268, corresponding to $M^{+\bullet}$ of 16:1; (*C*) *m/z* 266, corresponding to $M^{+\bullet}$ of 16:2; and (*D*) *m/z* 264, corresponding to $M^{+\bullet}$ of 16:3. The specific products of *M. sexta* FADs were identified as *E*11-14:1 (2), *Z*11-14:1 (3), *E*11-16:1 (5), *Z*11-16:1 (6), *Z*11,*E*13-16:2 (11), *E*10,*Z*12-16:2 (12), *E*10,*E*12-16:2 (14), *E*10,*E*12,*E*14-16:3 (15), and *E*10,*E*12,*Z*14-16:3 (16). Additionally, nonspecific, yeast-produced FAs were detected in all yeast strains: *Z*9-14:1 (1), *Z*9-16:1 (4), traces of *Z*11-16:1 (6), and unidentified compounds (10) and (13). In yeast expressing *Msex*D3, *E*13-16:1 (7), *Z*13-16:1 (8), and *Z*11,*E*13-16:2 (11) were identified as products of yeast fatty acid elongase acting on *Z*11-14:1 and *E*11-14:1. Cultivation media for yeasts cultivated for analysis of 14:1 were supplemented with 14:0, media were supplemented with *Z*11-16:1 for analysis of 16:2, and media were supplemented with *E*10,*E*12-16:2 for analysis of 16:3, as described in *Materials and Methods*. For a detailed analysis of nonspecific products, see *SI Appendix*, Fig. S4.

and products of FADs involved in 3UFA-derived SPC biosynthesis, we topically applied metabolic probes in the form of FAs and FAMEs to female *M. sexta* PGs. Deuterium-labeled *E*10,*E*12-16,16,16-$^{2}H_3$-16:2 methyl ester (further referred to as d3-*E*10,*E*12-16:2) applied to PGs was incorporated into two d3-16:3 FAME isomers. Based on the reduction in their retention times compared with the nondeuterated 3UFA methyl ester standards [consistent with the inverse isotopic effect (23)], we identified them as d3-*E*10,*E*12,*E*14-16:3 and d3-*E*10,*E*12,*Z*14-16:3, thus confirming the biosynthesis of 3UFAs from *E*10,*E*12-16:2 in vivo (*SI Appendix*, Figs. S8 and S9).

The identification of *E*11-14:1 and *Z*11-14:1 in the *Msex*D3-expressing yeast strain was confirmed in vivo by incorporation of topically applied 1,2-$^{13}C_2$-tetradecanoic acid into $^{13}C_2$-*Z*11-14:1 and $^{13}C_2$-*E*11-14:1 in the AT. Although they can be biosynthesized in vivo, *Z*11-14:1 and *E*11-14:1 are not naturally present in the *M. sexta* AT, likely due to the low abundance of 14:0 available in AT (*SI Appendix*, Figs. S9 and S10 and ref. 24).

Additionally, we detected *Z*11,*E*13-16:2 in the untreated *M. sexta* AT (*SI Appendix*, Fig. S11), which had not previously been detected in the FA pool of the *M. sexta* PG (24) and which we found to be specifically produced in yeast expressing *Msex*D5 (Fig. 2).

Together, the functional characterization of isolated FADs in our yeast expression system combined with the application of metabolic probes and analysis of FAs indicates that 3UFAs are biosynthesized in *M. sexta* AT by either of the two distinct desaturases *Msex*D3 or *Msex*D5, which share *E*/*Z*14-desaturase specificity but differ in their other desaturase products (Fig. 3).

Reconstruction of the Phylogenetic Relationship Between *M. sexta* and Other Lepidopteran FADs. We reconstructed a FAD gene tree using publicly available sequences of predicted or functionally characterized lepidopteran FADs, 14 FAD genes predicted from the *M. sexta* Official Gene Set 2.0 and additional moth FAD sequences available from in-house sequencing projects (Fig. 4, Dataset S2, and *SI Appendix*, Table S2).

The FAD gene tree exhibits several well-supported clades. The most sequentially and functionally conserved clades are those of Z9-FADs, that is, a clade of FADs that prefer palmitic acid over stearic acid (16:0 > 18:0) that includes the previously characterized *Msex*D1 (18), and a FAD clade that prefers stearic acid (18:0 > 16:0) that includes the predicted *Msex*D4. Both *Msex*D3 and *Msex*D5 cluster within a variable clade of SP-biosynthetic FADs herein termed "Z11-like," which encompasses highly functionally diverse pheromone biosynthetic FADs (25), in addition to numerous FADs with Z11-desaturase specificity. Of note, the closest putative *Msex*D5 ortholog is desat1 from *Ascotis selenaria*, which is proposed to be a nonfunctional FAD (26). Putative orthologs of *Msex*D5 are predicted also in other moth species that do not possess 3UFA SPCs (e.g., the pine caterpillar moth *Dendrolimus punctatus* and the silkworm moth *Bombyx mori*) (Fig. 4).

The closest homolog of *Msex*D3 is *Msex*D2, indicating that the duplication event leading to the tandemly arranged gene pair of *Msex*D2 and *Msex*D3 occurred after separation of the *B. mori* and *M. sexta* lineages. Alternatively, *B. mori* could have lost the FAD gene orthologous to *Msex*D3. The former scenario, which proposes a more recent gene duplication event, is further supported by the high sequence identity of *Msex*D2 and *Msex*D3.

The phylogenetic reconstruction yielded six additional strongly supported clades (I–VI, Fig. 4). Typically, FADs from *M. sexta* and *B. mori* that are presumably not involved in SP biosynthesis are in clades orthologous to moth FADs for which involvement in SP biosynthesis was implied based on their experimentally determined desaturase specificity. The tree topology provides strong support for the hypothesis that biosynthetically inactive members of the FAD gene family are retained in the moth genomes and in the course of evolution can be activated and recruited for novel SPC biosynthesis (11).

Based on these results, we propose that the recruitment of *Msex*D3 and *Msex*D5 genes for SPC biosynthesis occurred after separation of the *M. sexta* and *B. mori* lineages and led to the acquisition of 3UFA SPC precursors in *M. sexta*, thus extending

Fig. 3. The reconstructed desaturation pathway of *M. sexta* SPC precursors compared with that of *B. mori*. (*A*) In *M. sexta*, the desaturation pathway is extended by an *E*/*Z*14-desaturation step catalyzed by *Msex*D3 and/or *Msex*D5, which leads to 3UFA SPC precursors. Desaturase specificities of *Msex*D2 and *Msex*D6 contribute to additional precursors of minor SPCs. (*B*) Biosynthesis of the SPC precursor *E*10,*Z*12-16:2 in *B. mori* (44). Precursors of SPCs essential for triggering the full range of male premating responses are framed in green (27, 45).

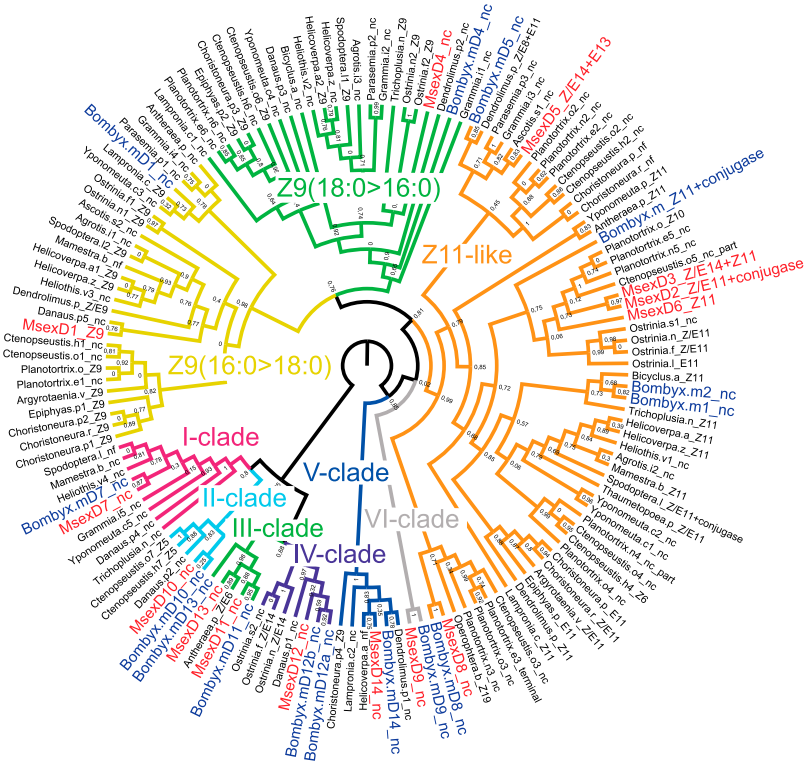

Fig. 4. Phylogenetic tree showing the relationships between lepidopteran FADs. *M. sexta* desaturases are highlighted in red. *B. mori* desaturases are highlighted in blue. Eight highly supported clades are colored and named. FADs are named by the genus and a single letter abbreviation of the source species name followed by designation of the FAD specificity, when available, or by "nc" for FADs that have not been functionally characterized or "nf" for FADs that were functionally assayed but no desaturase activity was detected. Numbers along branches indicate branch support calculated by approximate likelihood ratio test (aLRT, minimum of SH-like and Chi2-based values). For GenBank sequence accession numbers and full species names, see *SI Appendix*, Table S2.

the SP biosynthetic pathway by an additional *E*/*Z*-14 desaturation step compared with *B. mori* (Fig. 3).

We identified 3UFAs also in the AT of the death head moth, *Acherontia atropos* (Sphinginae: Acherontiini; *SI Appendix*, Fig. S12 and *SI Appendix*, *SI Materials and Methods*). This finding places the most parsimonious recruitment of 3UFA-producing FADs in the common ancestor of the Acherontiini and Sphingiini tribes, the Sphinginae subfamily (*SI Appendix*, Fig. S13 and Table S3).

Identification of the Sequence Determinants of *E*/*Z*14-Desaturase Specificity in *Msex*D3. To identify the domains, structural motifs, and amino acid residues critical for the distinct specificities of *Msex*D2 and *Msex*D3, we prepared a set of truncated, domain-swapped and single-amino acid-swapped mutants of *Msex*D2 and *Msex*D3 (Fig. 5*A*). Mutated FADs were expressed in *S. cerevisiae*, and total yeast cell FAs were analyzed. To assess the effect of individual mutations on the desaturase specificity, we determined the relative amounts of major pheromone precursors (*Z*11-16:1, *E*10, *Z*12-16:2, *E*10,*E*12-16:2, *E*10,*E*12,*E*14-16:3, and *E*10,*E*12,*Z*14-16:3) produced by the *Msex*D2 and *Msex*D3 mutants.

To test the role of variable N- and C-terminal regions on desaturase specificity, we prepared a set of truncation mutants. The identification of 3UFA products in the *Msex*D3-C20 mutant, truncated by 20 amino acids from the C terminus, indicated the dispensability of this extension for *E*/*Z*14-desaturase specificity. Additional 20 amino acids truncation (*Msex*D3-C40) led, however, to complete loss of both *Z*11- and *Z*/*E*14-desaturase activities, suggesting that the extensive deletion affected the general desaturase activity of *Msex*D3 (Fig. 5). The truncation of both desaturases by 14 amino acids at the N terminus (*Msex*D2-N14, *Msex*D3-N14) did not change the spectrum of desaturase products (Fig. 5).

Besides the N- and C-terminal regions, the protein sequence divergence between *Msex*D2 and *Msex*D3 is concentrated in the hydrophobic region between the first two histidine motifs (HR, Leu98–Val118) and in the fourth putative transmembrane domain (TM4, Trp210–Ala231) (*SI Appendix*, Fig. S1). Therefore, we reciprocally swapped the HR and TM4 regions, resulting in chimeric FADs (Fig. 5*A*). The exchange of the HR region did not change the desaturase product spectrum in the chimeras *Msex*D2-HR and *Msex*D3-HR (Fig. 5). However, the exchange of the *Msex*D2 TM4 domain with TM4 of *Msex*D3 (*Msex*D2-TM4 chimera) led to a fundamental change in *Msex*D2-TM4 products compared with *Msex*D2; the conjugase and *Z*11-desaturase specificity was almost completely abolished ($P < 0.05$). Notably, traces of *E*10,*E*12,*E*14-16:3 and *E*10,*E*12,*Z*14-16:3 were detected, indicating a gain of *E*/*Z*14-desaturase specificity in *Msex*D2-TM4 (Fig. 5). Together, these results indicate that the exchange of TM4 in *Msex*D2-TM4 led to an overall shift in desaturase specificity toward *Msex*D3. In a reciprocal fashion, *Msex*D3-TM4 exhibited an increase of *Z*11-16:1 production ($P < 0.05$) to a level of *Z*11-16:1 produced by *Msex*D2 (Fig. 5*B*), the acquisition of conjugase activity (Fig. 5*C*), and loss of *E*/*Z*14 specificity as indicated by loss of 3UFA products (Fig. 5*D*). Thus, *Msex*D3-TM4 displayed the full spectrum of *Msex*D2 products.

To determine the contribution of individual amino acid residues to the observed reciprocal exchange of desaturase specificities in TM4 mutants, we swapped individual nonconserved amino acids and generated mutants *Msex*D2-216, *Msex*D3-216, *Msex*D2-219, *Msex*D3-219, *Msex*D2-220, *Msex*D3-220, *Msex*D2-223, *Msex*D3-223, *Msex*D2-224, and *Msex*D3-224. The mutations at amino acid positions 216, 219, 220, and 223 either led to a decrease in desaturase activity ($P < 0.05$) or did not significantly change the overall desaturase activity ($P > 0.05$) and did not lead to production of novel desaturase products (Fig. 5). However, the exchange of alanine and isoleucine at residue 224 led to a reciprocal exchange of desaturase specificities similar to that observed for the TM4 exchange (Fig. 5). Notably, *Msex*D2-224Ile lost conjugase activity (Fig. 5*C*) and gained *E*/*Z*14-desaturase specificity, as indicated by production of *E*10,*E*12,*E*14-16:3 and *E*10,*E*12,*Z*14-16:3 (Fig. 5*D*), whereas *Msex*D3-224Ala completely lost the ability to produce 3UFAs (Fig. 5*D*) but acquired conjugase activity (Fig. 5*C*).

To control for the influence of different protein expression levels of *Msex*D2-224Ile- and *Msex*D3-224Ala- on specificity changes, we cloned these mutants in-frame with the N-terminal His6tag and detected their levels in yeast lysates using anti-His6tag antibodies. The FADs were produced at comparable levels and exhibited also reciprocal exchange of desaturase specificities (*SI Appendix*, Fig. S14).

Using homology modeling with mammalian FADs as a template (20, 21) we generated structural models of *Msex*D2 and *Msex*D3,

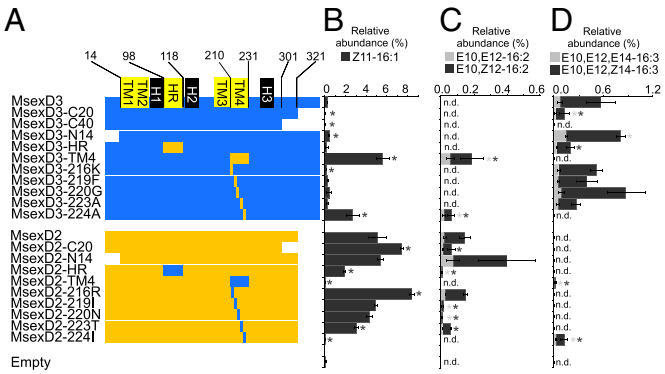

Fig. 5. Identification of sequence determinants of *Msex*D2 and *Msex*D3 desaturase specificities by site-directed mutagenesis. (*A*) Overview of truncated, domain-swapped, and single-amino-acid-swapped mutants. Predicted transmembrane helices (TM1–TM4), the hydrophobic region (HR), and conserved histidine motifs (H1–H3) are highlighted, and the amino acid positions of swapped or truncated regions are marked with numbers. (*B*) Relative amounts of *Z*11-16:1 accumulated in yeast strains expressing *Msex*D2 and *Msex*D3 mutants. (*C*) Relative amounts of *E*10,*E*12-16:2 and *E*10,*Z*12-16:2 accumulated in yeast strains expressing *Msex*D2 and *Msex*D3 mutants cultivated in the presence of *Z*11-16:1. (*D*) Relative amounts of *E*10,*E*12,*E*14-16:3 and *E*10,*E*12,*Z*14-16:3 accumulated in yeast strains expressing *Msex*D2 and *Msex*D3 mutants cultivated in the presence of *E*10,*E*12-16:2. The relative abundances of individual FAMEs were calculated from the peak areas in GC/MS chromatograms. Bars represent means ± SD of relative FAME abundances in three cultivation replicates. *Significant difference compared with the parental wild-type FAD (two-sample *t* test, $P < 0.05$, gray and black asterisks indicate the significant differences for each of the FAME isomers). n.d., FAME not detected. Empty, control yeast strain transformed with an empty plasmid.

which indicate that the residue 224 is contributing to the formation of the kink in fatty acyl substrate binding tunnel (*SI Appendix*, Fig. S15).

Together, these findings provide evidence that a single amino acid substitution in *Msex*D2 is sufficient to abolish the original desaturase specificities and introduce an *E*/*Z*14-desaturase specificity, leading to the production of 3UFA SPC precursors.

Discussion

Using next-generation sequencing of *M. sexta* female PG and reference tissues, we identified a set of highly abundant and PG-enriched FAD transcripts, including *Msex*D2, a previously described FAD involved in biosynthesis of mono- and diunsaturated SPC precursors (18), and previously unidentified *Msex*D3, *Msex*D5, and *Msex*D6 FADs. The 3UFA precursor of the essential *M. sexta* SPC *E*10,*E*12,*Z*14-16:3-aldehyde (27), along with *E*10,*E*12,*E*14-16:3, was produced by *Msex*D3 and *Msex*D5 in our yeast expression system.

Under the hypothesis that both *Msex*D3 and *Msex*D5 are biosynthetically active in vivo, the biosynthesis of 3UFA precursors of SPC would be redundantly catalyzed by two evolutionarily distinct enzymes, a feature that has not been previously described in SP-biosynthetic FADs. The selection pressure leading to the recruitment of a second, seemingly redundant, 3UFA-biosynthetic FAD might occur, for example, to secure a sufficiently high production of 3UFA-derived SPCs. However, our results suggest that *Msex*D3 plays the principal role in 3UFA biosynthesis because (*i*) *Msex*D3 transcript is more abundant in the PG compared with *Msex*D5 and (*ii*) the 1:7 ratio of *E*10,*E*12, *E*14-16:3 and *E*10,*E*12,*Z*14-16:3 produced by *Msex*D3 closely resembles the ratio of the respective aldehydic components in the *M. sexta* SP (approximately 1:10) (27), in contrast to the ratio of *Msex*D5 3UFA products (3:1).

The evolutionary events leading to the acquisition of *Msex*D5 are uncovered by the FAD gene family tree, which indicates several putative orthologs of *Msex*D5 across moth species. None of the orthologs exhibits *E*/*Z*14-desaturase specificity. Rather, they (*i*) are presumably not active in SP biosynthesis, such as desat1 from the Japanese giant looper *Ascotis selenaria* (26), (*ii*) exhibit distinct desaturase specificity, such as FAD from *Dendrolimus punctatus* (28), or (*iii*) have not been functionally characterized, such as putative FADs from *Grammia incorrupta* and *Parasemia plantaginis*. The reconstructed FAD gene tree suggests that *Msex*D5 was acquired by activation of an inactive FAD gene. This is further supported by the topology of the FAD gene tree containing well-supported clades I–VI, which typically encompass (in addition to presumably nonfunctional FADs or FADs not involved in SP biosynthesis) FADs exhibiting unique desaturase specificities. The rich FAD multigene family would thus serve as a reservoir from which novel SP-biosynthetic FADs can be recruited (7, 11).

Our finding of a single amino acid residue 224 that critically influences desaturase specificity of *Msex*D2 and *Msex*D3 is consistent with results obtained for other FADs from across kingdoms (20, 29–31), indicating high enzymatic plasticity of FADs, that is, susceptibility to shifts in their enzymatic specificities following a small number of amino acid substitutions. Homology models of *Msex*D2 and *Msex*D3 localizing the amino acid residue 224 (Ala and Ile, respectively) to position of conserved Thr257 in Z9-FADs, which contributes to formation of the kink in the FA substrate binding tunnel (20, 21), suggest that the kink determines the desaturase substrate specificity by positioning the fatty acyl chain in respect to the diiron active center (*SI Appendix*, Fig. S15). Future studies should show whether this mechanism of desaturase substrate selectivity is shared across FADs from various organisms. Additionally, our results together with the observed influence of one amino acid substitution on specificity of SP-biosynthetic FA reductases (8) and SP-receptor (32) in *Ostrinia* moths suggest an evolutionary significant effect of a single amino acid substitution in key proteins involved in pheromone communication on moth speciation.

In summary, we show that two distinct *E*/*Z*14-FADs (*Msex*D3 and *Msex*D5) are capable of biosynthesis of unique 3UFA SPC precursors in *M. sexta*. The *E*/*Z*14-desaturase specificity of *Msex*D3 could have evolved abruptly via a single amino acid mutation in a gene duplicate of 1UFA- and 2UFA-producing *Msex*D2. Alternatively, 3UFA SPCs might have been acquired in *M. sexta* via activation of presumably inactive ancestral *Msex*D5. These results indicate that the presence of inactive FAD genes in moth genomes and the susceptibility of FAD enzymes to changes of the desaturase specificity underlie an evolutionary facile recruitment of novel compounds for the SP communication channel.

Materials and Methods

For detailed descriptions see *SI Appendix, SI Materials and Methods*.

RNA Isolation. *M. sexta* females were reared under conditions described by Große-Wilde et al. (33). Total RNA was extracted from each of the adult and larval tissue samples.

Illumina Sequencing, Transcriptome Assembly, and Annotation. Tissue-specific transcriptome sequencing of four different mRNA pools was carried out on an Illumina HiSeq2000 Genome Analyzer platform. The transcriptome was annotated using BLAST, Gene Ontology and InterProScan searches using BLAST2GO PRO v2.6.1 (www.blast2go.de/) as described (34).

Digital Gene Expression Analysis. Digital gene expression analysis was carried out by using QSeq software (DNAStar Inc.). Biases in the sequence datasets and different transcript sizes were corrected using the RPKM algorithm.

Sequence Analysis. Desaturase topology was predicted using the web-based program TMHMM 2.0 (35). Maximum-likelihood phylogenetic analysis was performed in the web-based pipeline Phylogeny.fr (36) using protein sequences of lepidopteran FADs retrieved from the EMBL database, ManducaBase (www.agripestbase.org), SilkBase (silkbase.ab.a.u-tokyo.ac.jp), and in-house sequencing projects.

Desaturase Cloning. A cDNA library used for isolation of FAD ORFs was prepared from total RNA extracted from ATs, consisting of PG, papillae anales, and intersegmental membranes, of female *M. sexta*. FAD ORFs were cloned into the pYES2 (Invitrogen) or pYEXTHS-BN vector. pYEXTHS-BN plasmids encoded FADs with N-terminal His6tags. Vectors bearing mutated *Msex*D2 or *Msex*D3 were constructed as described in detail in *SI Appendix, SI Materials and Methods*.

Functional Expression in Yeast. Yeasts transformed with pYES2 and pYEXTHS-BN were cultivated in liquid YNB medium lacking uracil. Heterologous FAD expression in pYEXTHS-BN transformed yeasts was monitored by Western blotting using anti-His6tag antibodies (37). Total cellular lipids were transesterified to FAMEs (18). When indicated, yeast strains were cultivated with FAMEs supplemented to a final concentration of 0.25 mM in cultivation medium.

GC/MS Analysis. The FAME extracts were analyzed by GC/MS (MasSpec-Micromass; EI at 70 eV) using DB-5MS and DB-WAX capillary columns (both from J&W Scientific). The double-bond positions of the FAMEs were determined by concordance of retention times and mass spectra of FAMEs in analyzed yeast extracts with that of synthetic UFA standards and by derivatization with MTAD and dimethyldisulfide.

Chemical Synthesis. The synthesis of methyl *E*10,*E*12,*Z*14-hexadecatrienoate was performed by a single-step Suzuki–Miyaura coupling (38). Methyl Z11,E13-hexadecadienoate was prepared by a Wittig reaction (39). Methyl *E*10,*E*12-hexadecadienoate was prepared by coupling methyl 11-undecynoate and (*E*)-iodo pentene (40). Methyl *E*10,*E*12-16,16,16-trideuteriohexadecadienoate was prepared by coupling methyl 11-undecynoate with (*E*)-2-((4-iodobut-3-enyl)oxy)tetrahydro-2H-pyran (41).

Application of Metabolic Probes to *M. sexta* AT. One microliter of *E*10,*E*12-16,16,16-$^{2}H_3$-16:2-methyl ester (50 μg/μL) or 1,2-$^{13}C_2$-14:0 acid (50 μg/μL; Sigma-Aldrich) in dimethyl sulfoxide/water/ethanol (7/2/1) was applied topically to *M. sexta* ATs. ATs were dissected after 24 h, extracted, and analyzed by GC/MS (42).

Homology Modeling. The structures of *Msex*D2 and *Msex*D3 were generated using homology modeling module in YASARA (43) with default parameters. Structures of mammalian FADs (PDB ID codes 4YMK and 4ZYO) were used as templates.

ACKNOWLEDGMENTS. We thank Sylke Dietel and Christopher Koenig for *M. sexta* rearing, Jan Doubský for assistance in fatty acid methyl ester organic synthesis (all Max Planck Institute for Chemical Ecology), Rikard Unelius (Linnaeus University) for providing *Z*11,*E*13-16:2 standard, Vladimír Vrkoslav for technical assistance with GC/MS analyses and Michal Doležal (both Institute of Organic Chemistry and Biochemistry) for generating the FAD homology models, Caterina Holz for providing the pYEXTHS-BN plasmid, and Hillary Hoffman for language consulting. This research was financially supported by project RVO 61388963 from Academy of Sciences of the Czech Republic, project LO 1302 from Ministry of Education of the Czech Republic and by the Max Planck Society. P.M. was supported by the European Social Fund and the state budget of the Czech Republic (Project CZ.1.07/2.3.00/30.0022).

1. Johansson BG, Jones TM (2007) The role of chemical communication in mate choice. *Biol Rev Camb Philos Soc* 82(2):265–289.
2. Paterson HEH (1985) The recognition concept of species. *Species and Speciation*, ed Vrba ES (Transvaal Museum, Pretoria, South Africa).
3. Phelan PL (1992) Evolution of sex pheromones and the role of asymmetric tracking. *Insect Chemical Ecology: An Evolutionary Approach*, eds Roitberg BD, Isman MB (Chapman & Hall, New York), pp 265–314.
4. Smadja C, Butlin RK (2009) On the scent of speciation: The chemosensory system and its role in premating isolation. *Heredity (Edinb)* 102(1):77–97.
5. Niehuis O, et al. (2013) Behavioural and genetic analyses of *Nasonia* shed light on the evolution of sex pheromones. *Nature* 494(7437):345–348.
6. Shirangi TR, Dufour HD, Williams TM, Carroll SB (2009) Rapid evolution of sex pheromone-producing enzyme expression in *Drosophila*. *PLoS Biol* 7(8):e1000168.
7. Roelofs WL, et al. (2002) Evolution of moth sex pheromones via ancestral genes. *Proc Natl Acad Sci USA* 99(21):13621–13626.
8. Lassance J-M, et al. (2013) Functional consequences of sequence variation in the pheromone biosynthetic gene pgFAR for *Ostrinia* moths. *Proc Natl Acad Sci USA* 110(10):3967–3972.
9. Groot AT, et al. (2014) Within-population variability in a moth sex pheromone blend: Genetic basis and behavioural consequences. *Proc Biol Sci* 281(1779):20133054.
10. El-Sayed (2014) The Pherobase: Database of Pheromones and Semiochemicals. Available at www.pherobase.com.
11. Roelofs WL, Rooney AP (2003) Molecular genetics and evolution of pheromone biosynthesis in Lepidoptera. *Proc Natl Acad Sci USA* 100(16):9179–9184.
12. Jurenka RA, Haynes KF, Adlof RO, Bengtsson M, Roelofs WL (1994) Sex pheromone component ratio in the cabbage looper moth altered by a mutation affecting the fatty acid chain-shortening reactions in the pheromone biosynthetic pathway. *Insect Biochem Mol Biol* 24(4):373–381.
13. Tabata J, Ishikawa Y (2005) Genetic basis to divergence of sex pheromones in two closely related moths, *Ostrinia scapulalis* and *O. zealis*. *J Chem Ecol* 31(5):1111–1124.
14. Wang H-L, Liénard MA, Zhao CH, Wang CZ, Löfstedt C (2010) Neofunctionalization in an ancestral insect desaturase lineage led to rare Δ6 pheromone signals in the Chinese tussah silkworm. *Insect Biochem Mol Biol* 40(10):742–751.
15. Xue B, Rooney AP, Kajikawa M, Okada N, Roelofs WL (2007) Novel sex pheromone desaturases in the genomes of corn borers generated through gene duplication and retroposon fusion. *Proc Natl Acad Sci USA* 104(11):4467–4472.
16. Fujii T, et al. (2011) Sex pheromone desaturase functioning in a primitive *Ostrinia* moth is cryptically conserved in congeners' genomes. *Proc Natl Acad Sci USA* 108(17):7102–7106.
17. Albre J, et al. (2012) Sex pheromone evolution is associated with differential regulation of the same desaturase gene in two genera of leafroller moths. *PLoS Genet* 8(1):e1002489.
18. Matousková P, Pichová I, Svatoš A (2007) Functional characterization of a desaturase from the tobacco hornworm moth (*Manduca sexta*) with bifunctional Z11- and 10,12-desaturase activity. *Insect Biochem Mol Biol* 37(6):601–610.
19. Fang N, Teal PEA, Doolittle RE, Tumlinson JH (1995) Biosynthesis of conjugated olefinic systems in the sex pheromone gland of female tobacco hornworm moths, *Manduca sexta* (L.). *Insect Biochem Mol Biol* 25(1):39–48.
20. Bai Y, et al. (2015) X-ray structure of a mammalian stearoyl-CoA desaturase. *Nature* 524(7564):252–256.
21. Wang H, et al. (2015) Crystal structure of human stearoyl-coenzyme A desaturase in complex with substrate. *Nat Struct Mol Biol* 22(7):581–585.
22. Schneiter R, Tatzer V, Gogg G, Leitner E, Kohlwein SD (2000) Elo1p-dependent carboxy-terminal elongation of C14:1Delta(9) to C16:1Delta(11) fatty acids in *Saccharomyces cerevisiae*. *J Bacteriol* 182(13):3655–3660.
23. Shi B, Davis BH (1993) Gas chromatographic separation of pairs of isotopic molecules. *J Chromatogr A* 654(2):319–325.
24. Tumlinson JH, Teal PE, Fang N (1996) The integral role of triacyl glycerols in the biosynthesis of the aldehydic sex pheromones of *Manduca sexta* (L). *Bioorg Med Chem* 4(3):451–460.
25. Knipple DC, Rosenfield C-L, Nielsen R, You KM, Jeong SE (2002) Evolution of the integral membrane desaturase gene family in moths and flies. *Genetics* 162(4):1737–1752.
26. Fujii T, et al. (2013) Discovery of a disused desaturase gene from the pheromone gland of the moth *Ascotis selenaria*, which secretes an epoxyalkenyl sex pheromone. *Biochem Biophys Res Commun* 441(4):849–855.
27. Tumlinson JH, et al. (1989) Identification of a pheromone blend attractive to *Manduca sexta* (L.) males in a wind tunnel. *Arch Insect Biochem Physiol* 10(4):255–271.
28. Liénard MA, et al. (2010) Elucidation of the sex-pheromone biosynthesis producing 5,7-dodecadienes in *Dendrolimus punctatus* (Lepidoptera: Lasiocampidae) reveals Delta 11- and Delta 9-desaturases with unusual catalytic properties. *Insect Biochem Mol Biol* 40(6):440–452.
29. Lim ZL, Senger T, Vrinten P (2014) Four amino acid residues influence the substrate chain-length and regioselectivity of Siganus canaliculatus Δ4 and Δ5/6 desaturases. *Lipids* 49(4):357–367.
30. Meesapyodsuk D, Qiu X (2014) Structure determinants for the substrate specificity of acyl-CoA Δ9 desaturases from a marine copepod. *ACS Chem Biol* 9(4):922–934.
31. Rawat R, Yu XH, Sweet M, Shanklin J (2012) Conjugated fatty acid synthesis: Residues 111 and 115 influence product partitioning of *Momordica charantia* conjugase. *J Biol Chem* 287(20):16230–16237.
32. Leary GP, et al. (2012) Single mutation to a sex pheromone receptor provides adaptive specificity between closely related moth species. *Proc Natl Acad Sci USA* 109(35):14081–14086.
33. Große-Wilde E, et al. (2010) Sex-specific odorant receptors of the tobacco hornworm *manduca sexta*. *Front Cell Neurosci* 4:7.
34. Vogel H, Badapanda C, Knorr E, Vilcinskas A (2014) RNA-sequencing analysis reveals abundant developmental stage-specific and immunity-related genes in the pollen beetle *Meligethes aeneus*. *Insect Mol Biol* 23(1):98–112.
35. Krogh A, Larsson B, von Heijne G, Sonnhammer EL (2001) Predicting transmembrane protein topology with a hidden Markov model: application to complete genomes. *J Mol Biol* 305(3):567–580.
36. Dereeper A, et al. (2008) Phylogeny.fr: Robust phylogenetic analysis for the non-specialist. *Nucleic Acids Res* 36(Web Server issue):W465–W469.
37. Buček A, Matoušková P, Sychrová H, Pichová I, Hrušková-Heidingsfeldová O (2014) Δ12-Fatty acid desaturase from *Candida parapsilosis* is a multifunctional desaturase producing a range of polyunsaturated and hydroxylated fatty acids. *PLoS One* 9(3):e93322.
38. Frost CG, Penrose SD, Gleave R (2008) Rhodium catalysed conjugate addition of a chiral alkenyltrifluoroborate salt: the enantioselective synthesis of hermitamides A and B. *Org Biomol Chem* 6(23):4340–4347.
39. Oonishi Y, Mori M, Sato Y (2007) Rhodium(I)-catalyzed intramolecular hydroacylation of 4,6-dienals: Novel synthesis of cycloheptenones. *Synthesis (Stuttg)* 2007(15):2323–2336.
40. Gagnon D, Lauzon S, Godbout C, Spino C (2005) Sterically biased 3,3-sigmatropic rearrangement of azides: Efficient preparation of nonracemic α-amino acids and heterocycles. *Org Lett* 7(21):4769–4771.
41. Stille JK, Simpson JH (1987) Stereospecific palladium-catalyzed coupling reactions of vinyl iodides with acetylenic tin reagents. *J Am Chem Soc* 109(10):2138–2152.
42. Svatoš A, Kalinová B, Boland W (1999) Stereochemistry of lepidopteran sex pheromone biosynthesis: A comparison of fatty acid-CoA Δ11-(Z)-desaturases in *Bombyx mori* and *Manduca sexta* female moths. *Insect Biochem Mol Biol* 29(3):225–232.
43. Krieger E, et al. (2009) Improving physical realism, stereochemistry, and side-chain accuracy in homology modeling: Four approaches that performed well in CASP8. *Proteins* 77(Suppl 9):114–122.
44. Moto K, et al. (2004) Involvement of a bifunctional fatty-acyl desaturase in the biosynthesis of the silkmoth, *Bombyx mori*, sex pheromone. *Proc Natl Acad Sci USA* 101(23):8631–8636.
45. Butenandt A, Beckmann R, Stamm D, Hecker E (1959) Über den sexuallockstoff des seidenspinners *Bombyx mori*. Reindarstellung und konstitution. *Z Naturforsch B* 14:283–284.